Research Square

Preprints are preliminary reports that have not undergone peer review.
They should not be considered conclusive, used to inform clinical practice,
or referenced by the media as validated information.

# Pithoascus kurdistanensis: Discovery of a Novel Endophytic Fungal Species Associated with Papaver bracteatum, and its Production of Morphine Compounds

**Sima Mohammadi**
Université Laval Québec
**Bahman Bahramnejad**
University of Kurdistan
**Jafar Abdollahzadeh**
University of Kurdistan
**Samaneh Bashiri**
University of Kurdistan
**Antony T. Vincent**
Université Laval Québec
**Mohammad Majdi**
University of Kurdistan
**Jalal Soltani**
Bu-Ali Sina University
**Roger C. Levesque**
rclevesq@ibis.ulaval.ca

Université Laval Québec

**Article**

**Keywords:** Microascaceae, Pithoascus, Papaver, Morphinan alkaloids, HPLC, GC/MS

**Posted Date:** May 6th, 2024

**DOI:** https://doi.org/10.21203/rs.3.rs-4018361/v1

**License:** This work is licensed under a Creative Commons Attribution 4.0 International License. Read Full License

**Additional Declarations:** No competing interests reported.

**Version of Record:** A version of this preprint was published at Scientific Reports on September 30th, 2024. See the published version at https://doi.org/10.1038/s41598-024-71344-z.

## Abstract

*Papaver* genus, commonly known as popies, is a valuable source of alkaloids used in medicine, including papaverine, morphine, codeine, and thebaine. We isolated six endophytic fungal isolates producing morphinan alkaloids from four *Papaver* species growing in Kurdistan Province, Iran. To do this, a 1:1 mixture of methanol and chloroform was used to extract fungal cultures. The contents of morphinan alkaloids in the extracts were subsequently determined using phase high-performance liquid chromatography (HPLC). Among the morphinan alkaloid-producing fungal isolates, IRAN 4653C had the highest yield giving 23.06 (Mg/g) morphine and 2.03 (Mg/g) codeine when grown in potato dextrose liquid medium. Moreover, the morphinan productivity of IRAN 4653C was further validated by gas chromatography-mass spectrometry (GC-MS). The identity of this isolate was examined and recognized as a new fungal species named as *Pithoascus kurdistanesis* sp. nov. based on multi-gene phylogenetic analyses of ITS, TEF-1α, and TUB2 sequence data and morphological features. The morphinan-producing endophytic fungus and the isolated *Pithoascus* species from *Papaver* are being reported for the first time. Accordingly, this fungus shows promise as a new source of valuable compounds which is illustrated and introduced here as a new *Microascaceae* member belonging to *Pithoascus* from Kurdistan Province, Iran.


## Introduction

Benzylisoquinoline alkaloids (BIAs) are a group of specialized metabolites found in plants of the order Ranunculales, specifically in families like *Papaveraceae*. These compounds contain nitrogen and have various biological activities [1]. As secondary metabolites, BIAs are not crucial for normal growth and development, but they do play a crucial role in protecting plants against herbivores and pathogens. [2]. Tyrosine as a precursor of BIAs exhibits a wide range of pharmacological activities [3]. One subclass of benzylisoquinoline alkaloids is morphinan alkaloids, which are potent analgesics that have been used for thousands of years. These alkaloids are exclusively produced in plants of the *Papaver* genus. [4]. The *Papaver* genus is renowned for its production of various BIAs, including the potent painkiller morphine, the cough suppressant codeine, the muscle relaxant papaverine, an intermediate used in the semi-synthesis of other pentacyclic morphinan-based drugs, and the anti-microbial compound sanguinarine [5]. Nowadays, morphine and codeine continue to be the most beneficial and efficient compounds in medicine worldwide [6]. The intricate structures of morphinan, with five chiral centers, highlight the uneconomic commercial synthesis and cultivation of poppy as the most effective method for producing opiate analgesics [7].

*Papaver* as a genus (commonly known as poppy) belongs to the *Papaveraceae* family containing 830 species. These species are primarily found in temperate regions of the Northern Hemisphere, South Africa, and southern America [8]. Cullen (1966) reported 26 species of *Papaver*, including 5 that were endemic to Iran. However, this report did not take into account the sectional classification of the genus. More recent reports have identified species of this genus in various floristic regions of Iran [9,10] *Papaver* species can produce more than 170 different alkaloids, mainly in the form of benzylisoquinoline alkaloids (BIAs).

Endophytes constitute any kind of organism that colonizes healthy plant tissue intercellularly and/or intracellularly, apparently without causing visible damage or morphological changes [11]. It is known that endophytic fungi live inside their host plant for protracted periods of time; the earliest records of them date back 400 million years. [12]. Endophytic fungi are a valuable and reputable source of bioactive and novel compounds with immense potential in the fields of medicine and agriculture. They also play a crucial role in enhancing the ecological adaptability of their host plants [13,14]. Interactions between plants and fungi can increase the production of bioactive metabolites in medicinal plants [15]. Also, some specified endophytic fungi mimic the host plant's secondary metabolites profile and tend to produce the plant medicinal products [16,17] such as taxol, camptothecin, and its structural analogs [18], ginkgolide [19]. Therefore, researchers focusing on the isolation of endophytic fungi from pharmaceutical plants can discover many undescribed endophytic fungi species. Many

of these fungi possess the ability to produce a diverse range of secondary metabolites that are associated with plants, exhibiting a wide array of biological activities.

Endophytic fungi are frequently found within their host's metabolic networks, leading to changes in metabolite production and an increase in the presence of active compounds in medicinal plants [20] The evaluation of endophytic fungi plays a significant role in the production of bioactive metabolites which allows them to effectively adapt to their host and perform certain functions like synthesizing chemical compounds within these plants [21]. Researchers believe that the reason why endophytes produce certain chemical compounds is that genetic recombination occurred during evolution between the endophyte and its host [22,23]. This is the theory that was originally presented as an explanation for why the endophytic fungus *Taxomyces andreanae* should produce taxol [24]. Endophytic fungi in comparison with plants, grow much faster and are more appropriate for metabolic engineering [25]. Also, easier metabolites extraction from fungi could be valuable from both ecological and economic standpoints [24].

During a study on endophytic fungi associated with *Papaver* species and their secondary metabolite profiles for morphine alkaloids, we found a morphinan producing endophytic fungus placed in *Pithoascus* genus based on phylogenetic analyses of three loci (ITS, TEF-1α, TUB2) sequence data and morphological features.

*Pithoascus* was established by Von Arx (1973) based on the type species *P. nidicola*, which formerly included in *Microascus*[26]. Some researchers based on morphology considered this genus as a synonym with *Microascus* but reinstated by Sandoval-Dennis et al. (2016) [27–30] based on a multi-gene (LSU, ITS, TEF-1α, TUB2) phylogenetic study. *Pithoascus* is a member of the Microascaceae family and is distinguished by ascomata with simple or barely noticeable ostioles and navicular to fusiform ascospores devoid of germ pores. Asexual morph produced in some species with single and laterally annellidic conidiogenous cells and globose to pyriform 1-celled solitary conidia [30].

According to Indexfungorum (June 2023; www.indexfungorum.org) and Mycobank (www.mycobank.org) nine species have been introduced in *Pithoascus*. These species are associated with humans (hair, nail, tinea plantaris), rat (*Dipodomys merriami*), wasps (*Megachile willughbiella, Osmia rufa*), soil and plants (e.g. *Beta vulgaris*, *Fragaria vesca*, *Ferula ovina*) as saprophyte, endophyte and potential pathogen [30–32].

Here we introduce an endophytic fungus within *Pithoascus* genus as a new species and a taxonomic novelty for science which is able to produce morphinan species. This finding indicates the importance of microbial community associated with *Papaver* species as microbial potential sources to discover and produce new and valuable secondary metabolites.

# Results

- Isolation of fungi

We collected 17 endophytic fungal isolates from *P. bracteatum*, *P. glaucum, P. fugax*, and *P. argemone* grown in the Kurdistan Province, west of Iran, of which 13 isolates were from roots, three from capsules and one from stems. To study secondary metabolite profiles of endophytic fungi for producing morphinan alkaloids, 6 strains (BR4, BR6, GR1, GR4, PR1 and PS1) with more differences in morphological features were selected.

- Screening of fungal extracts for morphinan alkaloids

The extracts of all selected strains under the same condition were screened by HPLC to detect fungal morphinan compounds. The results showed that the peak positions and shapes of the selected fungi closely matched those of the chemical references for morphine, demonstrating that all the distinct fungi produced morphine.

Among the examined isolates, the highest yield of morphine (21.33 mg/g) and codeine (2.03 mg/g) was detected in BR6 whereas BR4 and PS1 contained lower yield of morphine (2.76 mg/g) and (0.18 mg/g), respectively. The GR1 extract contained morphine only (Table 3). Based on these results, BR6 was identified as the best strain to produce morphinan.

By GC/MS confirmation of BR6 as a morphinan producing endophytic fungus, authentic papaverine and morphine yielded at 22.222 and 22.090 Retention Time (min) respectively. Also, this analysis indicated that BR6 produced 30 volatile compounds which were identified and described by their molecular structures, functions, and the time of leaching identified by peaks (Table 4). Among several detected alkaloids papaverine has the highest percentage.

In addition to alkaloids, some compounds were detected in BR6 extract, most produced by Papaver species and other plants as secondary metabolites. For example, heptadecane, epi-bicyclosesquiphellandrene, delta-Cadinene naphthalene, ethofumesate, 2-ethylacridine, 4H-pyrane-3-carboxamide, ethidimuron, and hexadecanoic acid are some plants metabolites with antibacterial, anticancer, pesticide, herbicide, and antioxidant efficacy which were produced by BR6 (Table 4). These results can confirm the remarkable similarity between the endophytic fungi and *P. bracteatum* in terms of producing secondary metabolites [33–37].

- Characterization of selected morphinan producing fungus

The best morphinan producing fungal isolate (BR6) selected to study in more details was deposited in the culture collection of the Iranian Research Institute of Plant Protection, IRAN, Tehran, Iran (IRAN 4653C) and the Centraalbureau voor Schimmelcultures, CBS, Utrecht, The Netherlands (CBS 149789). The identity of the selected isolate IRAN 4653C studied based on multi-gene phylogenetic analyses and morological features.

- Phylogenetic analysis

Megablast search of NCBIs GenBank nucleotide database, with the ITS and TUB sequences gave closest hits to *Pithoascus intermedius* CBS 217.32 (ITS: 99.6%, 494/498, GenBank NR_132953; TUB: 94.2%, 455/483, 2 gaps, GenBank LM652662) and *Pithoascus nidicola* CBS 197.61 (95%, 511/538, 12 gaps, GenBank MH858021; TUB: 95.7%, 429/448, 1 gap, GenBank LM652663), and using TEF1-α sequence the closest hits were *Pithoascus intermedius* CBS 217.32 (96.6%, 926/959, 2 gaps, GenBank LM652579) and *Pithoascus stoveri* CBS 197.61 (97.5%, 935/959, 2 gaps, GenBank LM652581).

Sequences of our isolate IRAN 4653C were aligned with available authentic sequences of *Microascaceae* members (ITS: 37, TEF1-α: 28, TUB2: 29 sequences) and *Trichoderma asperellum* NBRC 101777 as outgroup retrieved from GenBank. Alignments for the ITS, TEF1-α, and TUB2 sequences including gaps contained 709, 976 and 601 characters, respectively. Single gene phylogenies confirmed the same phylogenetic position for our isolate and placed it within the genus *Pithoascus* (Figs S1–S3). The combined alignment of three loci including gaps contained 2288 characters, of which 164 were variable and parsimony uninformative, and 1375 were unvariable. Following a heuristic search of the remaining 749 parsimony informative characters, four trees with the same overall topology and the lowest parsimonious steps (CI = 0.47, HI = 0.53, RI = 0.64) were found.

The best nucleotide substitution model for all three loci (ITS, TEF1-α, TUB2) is the general time-reversible model of evolution (Rodríguez et al., 1990) according to MrModelTest. This model assumes a discrete gamma distribution (GTR+I+G) with six rate categories (lsetnst = 6, rates = invgamma), dirichlet (1,1,1,1) base frequencies, and includes estimation of invariable sites. 194 trees were removed as burn-in from the 782 trees that were produced by the Bayesian analysis of the concatenated alignments of three loci. The remaining 588 trees were used to calculate the consensus tree and posterior probability values (PP). By the end of the run, the average standard deviation of split frequencies was 0.009567. The Bayesian tree with similar topology as the trees resulting from MP analysis is shown in Figure 2-4. Using bootstrap support values at the nodes and BI/MP posterior probabilities, the MP tree was mapped onto a Baysian tree. In both MP and BI analyses our isolate IRAN 4653C clustered in *Pithoascus* genus separated from all known species

in a well-supported clade close to *P. intermedius*, *P. exsertus* and *P. nidicola*. Based on nucleotide sequences of examined three loci our isolate is differed from all three closely related species *P. intermedius* (ITS: 2 substitutions, 2 deletions/insertions; TEF1-α: 33 substitutions; TUB2: 33 substitutions, 1 deletion/insertion), *P. exsertus* (ITS: 35 substitutions; 21 deletions/insertions; TEF1-α: 38 substitutions, 1 deletion/insertion; TUB2: 43 substitutions; 4 deletions/insertions) and *P. nidicola* (ITS: 27 substitutions, 5 deletions/insertions; TEF1-α: 38 substitutions; TUB2: 25 substitutions, 1 deletion/insertion) and distinguished as a new species for science and named here as *Pithoascus kurdistanensis* sp. nov.

Taxonomy and nomenclature

***Pithoascus kurdistanensis*** Mohammadi S., Bahramnejad B. & Abdollahz. **sp. nov.** Fig. 2

**MycoBank** MB849386

**Etymology.** Name refers to Kurdistan Province, Iran, where this species was first found.

**Description.** Ascomata unpapillate, globose, pale to dark brown or black, semi-immersed or superficial, scattered or aggregated in dense crusts, covered with aerial hyphae, non-ostiolate, (67–) 80–120 (–243) µm, with a pseudoparenchymatous, layered, dark, thick-walled peridium. Setae aseptate or septate, straight or flexsuous, unbranched, pale to dark brown, (8–) 18–25 (–40) × 2–4 µm. Asci hyaline, globose, evanescent, 8-spored, (5–) 5.5–7.7 (–10) µm (av. ± S.D. = 6.9 ± 1.5). Ascospores conglobate inside the ascus, forming globose to sub-globose, small to large compact masses when asci disintegrate, hyaline at first, buff to olivaceous buff when mature, yellowish brown in mass, thin-walled, aseptate, navicular or lunate, often plano-convex, germ pores indistinct, (4.8–) 5.3–5.7 (–6.1) × (1.6–) 1.9–2.2 (–2.5) µm (av. ± S.D. = 5.5 ± 0.3 × 2 ± 0.2 µm). Conidiophores absent. Conidiogenous cells hyaline, cylindrical to ampulliform, rarely reduced to short swollen supporting cells, annellidic, smooth, rarely roughened and thin-walled, born singly, often laterally and rarely apically on aerial hyphae, (6–) 21–16 (–19) × (1.3–) 1.5–1.7 (–2.9) µm (av. ± S.D. = 13.2 ± 3.8 × 1.7 ± 0.4 µm). Conidia globose to pyriform, with a truncate base, smooth and thin-walled, aseptate, arranged in long basipetal dry chains, (3.3–) 3.5–5 (–5.7) × (2.8–) 3.5–4 (–4.5) µm (av. ± S.D. = 4.2 ± 0.7 × 3.6 ± 0.4 µm).

**Culture characteristics.** Colonies with appressed and immersed hyphae and aerial mycelium in the middle, whitish to pale grey. Colonies with daily rate less than 1 mm reaching 12, 10 and 10 mm diam on MEA, OA and PDA after 14 d at room temperature 20–25 °C.

**Typus.** IRAN, Kurdistan Province, Divandarreh, Saral region (35°33'57"N 46°48'47"E), *Papaver bracteatum*, 06 May 2018, H. Maroufi (holotype IRAN 18259F; ex-type strain IRAN 4653C = CBS 149789).

**Notes.** In multi-gene phylogeny, *Pithoascus kurdistanensis* placed close to *P. intermedius*, *P. exsertus* and *P. nidicola* in a clade distinct from all introduced species (Fig. 1). It is also distinguished from all other species in single-gene phylogenies based on ITS, *TEF-1α*, and *TUB2* sequences (Figs. S1-S3). Asexual morph in *P. exsertus* and *P. lunatus* and sexual morph in *P. ater* have not been reported. While most *Pithoascus* species (*P. intermedius*, *P. nidicola*, *P. stoveri*, *P. ater*) with known asexual morph produce solitary conidia on conidiogenous cells, *Pithoascus kurdistanensis* and *P. persica* produce conidia in long dry chains. Moreover, *P. kurdistanensis* is differentiated from closely related species *P. intermedius*, *P. nidicola* and *P. exsertus* by having smaller conidia, shorter ascospores and larger ascomata and ascospores, respectively (Table 5). This species is also separated from all described species by having setae, shape and size of asci (Table 5). Thus far, no setae have been reported in *Pithoascus* species. Main morphological characters useful for discriminating *Pithoascus* species are provided in table 5.

# Discussion

Endophytes often generate secondary metabolites that resemble those of their host plants. Because of this, they represent a very promising source of new bioactive compounds with a variety of possible biological uses [38]. A few studies have investigated endophytic microorganisms of *Papaver* species [39,40]. 2 bacterial endophytes that were recently isolated from various P. somniferum parts were studied for their capacity to increase resistance to a downy mildew [40]. Moreover, an endophytic fungus isolated from *P. somniferum* showed potential antimicrobial activities against four human bacterial pathogens and two fungi [41].

By confirmation of morphinan alkaloids presence in *P. glaucum*, *P. fugax*, *P. argemone*, and *P. bracteatum*, this study has been performed to investigate secondary metabolite profiles of associated endophytic fungi. There is the first report concerning the production of morphinan from endophytic fungi. HPLC results indicating the most potent endophytic fungal isolate in alkaloids production is IRAN 4653C which, isolated from the most efficient species of *Papaver* (*P. bracteatum*) in terms of producing morphine. Thus, it can be some similarities between endophytic fungus and its host. To further confirm, the IRAN 4653C production of morphinan was subjected to GC-MS high resolution analysis [42,43], in which addition to morphinan alkaloids, some plant metabolites are detected. Most of these compounds possess various biological activities, including antiviral, antimicrobial, anticancer, and antioxidant properties [33–35].

In terms of morphology, strain IRAN 4653C were related to genera of the *Microascaceae*. Various studies have been done to determine the best molecular markers for phylogenetic relationships of *Microascaceae* [20]. At the first step to clarify the identity of our isolate IRAN 4653C, we sequenced the internal transcribed spacer (ITS) region as a well-known universal DNA barcode marker in fungal phylogeny. BLAST analyses of ITS sequence data revealed that IRAN 4653C is closely related with *Pithoascus* species. The ITS, EF1-a, and TUB genes were the three loci sequenced in this study, which was conducted in response to a thorough investigation by Sandoval-Denis et al.[30]. Phylogenetic analyses of *Pithoascus* species were optimized using this multi-gene approach.

Based on multigene phylogenetic analyses strain IRAN 4653C placed in the genus *Pithoascus* distinct from all described species (i.e., *P. ater*, *P. exsertus*, *P. intermedious*, *P. lunatu*, *P. nidicola*, *P. persica*, and *P. stoveri*) and introduced here as a new species named *Pithoascus kurdistanensis* sp. nov. Main morphological characters useful in discrimination of *Pithoascus* species were determined and used to compare and discriminate strain IRAN 4653. Despite the overlap in morphological features, we can use a set of sexual/asexual morph characters together with phylogenetic analyses of sequence data to discriminate *Pithoascus* species. The most important character we documented in *P. kurdistanesis* is producing conidial chain in asexual morph as it is observed in morphology of *P. persica* which is not reported for *Pithoascus* species with asexual morph [29–31]. Moreover, we have seen setae in *P. kurdistanicus* for the first time in *Pithoascus* species. Thus, as the number of species and studied isolates around the world are growing, we will get clearer and roubust definition from the genus *Pithoascus* and species boundaries which contribute to revise the descriptions in future.

Microbial synthesis overcomes many of the obstacles complicated by using compounds produced in plants [44]. Thus, *P. kurdistanesis* IRAN 4653C could be an attractive alternative to plants for production alkaloids. Also, there is excellent potential in using *P. kurdistanesis* as a model system to investigate the new BIA biosynthesis pathways as a valuable source for the pharmaceutical industry. Additional studies addressing the completed genome sequence of the *P. kurdistanesis* and BIA biosynthetic pathway in this fungus will provide.

# Materials and Methods

- Sampling and fungal isolation

During April to May 2018, 4 different *Papaver* species; *P. bracteatum*, *P. glaucum*, *P. fugax*, and *P. argemone* were collected at flowering growth stage from different origins in Kurdistan Province, west of Iran. Disease-free plant samples were

surface sterilized and plated on Potato Dextrose Agar (PDA) with 100 mg/L ampicillin and streptomycin. Plates were incubated at 25 ˚C and monitored every day for growth of endophytic colonies and absence of saprophytic contamination. Following single-spore purification, the colonies were kept on PDA between 4 and 8 °C.

- Preparation of endophytic fungl extracts

Five (9 mm diameter) agar plugs of fungal isolates were inoculated in 500 mL flasks containing 200 mL of Potato Dextrose Broth (PDB) in the dark at 30 ˚C for 21 days on a rotary shaker (120 rpm). Then, flasks were kept in the dark at 25 ˚C under static conditions and fermented for 7 days. Methanol (MeOH) and chloroform (20:80 mL), two distinct solvents, were used for the extraction process in order to obtain both extracellular and intracellular secondary metabolites. 4 weeks later, the mycelia was removed from the culture by filtering it through 2 layers of cheesecloth. Each culture broth was given the same amount of organic solvent (1:1) to extract extracellular metabolites using this method. To remove waxy materials, the extract was placed at 4 ˚C for 12 hours. After gathering the organic phase, the solvent was extracted using a vacuum rotary evaporator set at 45°C. A final concentration of 250 mg/mL was achieved by dissolving the weighed residue in double distilled water. Lastly, a membrane with a 0.22 µm pore size was used to filter the concentrated extracts, which were then utilized in further experiments.

The mycelial biomass was harvested, washed thoroughly, and were macerated in 2X volume of solvents for 2 days on a rotary shaker. Next, a thorough homogenization of the mycelia was performed. The extracellular metabolites in the supernatants were further treated as previously explained. Before being utilized in bioassays, the secondary metabolites from every sample were kept at -20 ˚C.

- Analysis of extraction alkaloids by HPLC

The *Papaver* purified alkaloids were provided by Darou Pakhsh company, Tehran, Iran. For preparing the stock solution of standards, 1 mg was solved in MeOH. The alkaloid solution concentration series were made to calibrate the curves (morphine: 7.8–125.0 µg/ml; codeine: 7.8–125.0 µg/ml; thebaine 7.8–250.0 µg/ml; papaverine 7.8–250 µg/ml). The solution of plant samples and fungi samples were prepared and filtered with 0.45 µm diameter and transferred into HPLC vials and kept at the -20 ˚C until injection. An HPLC system with a C18 column (particle size 5 µm, 4 mm X 150 mm) and a Photo Diode Array Detector (PDA) was used to perform the HPLC analysis. The gradient mobile phase was solvent A (water) and B (acetonitrile) both of which contain 0.1% formic acid. The process of separation started with A and went from 100:0 to 85:15 in 20 minutes. It then reached 80:20 in 30 minutes, 65:35 in 40 minutes, and 100 B after a 10-minute column flush with 100% B. 280 nm was the wavelength used for detection. Every sample received two injections. The calibration curves for the standards were then made by plotting the peak areas against the concentrations.

- Gas chromatography-mass spectrometry (GC-MS)

The selected endophytic fungus extracts presumed to contain high amounts of morphinan compounds were analysed with gas chromatography/mass spectrometry (GC/MS) for validation. The fungus extract (0.5 mg) was transferred into a vial then added 1 of mL methanol and hydrochloric. The vial was vortexed and left at 50 ˚C for 12 hours and analyzed by GC-MS [45]. A 5977E MSD operating in EI mode at 70 eV was connected to an Agilent Technologies 7820A gas chromatograph, which was used to analyze 1 µl of the sample. The setup included a 30 m x 0.25 mm fused-silica capillary column with a stationary phase of 0.25 µm HP-5MS (Agilent Technologies, UK). The injection temperature was set at 270 ˚C and helium was used as the carrier gas at a constant flow rate of 1 ml/min. The temperature was then increased at a rate of 10 ˚C/min to 320 ˚C and held for 1 minute. For the analysis of polar compounds, a temperature program was used consisting of 2 minutes of isothermal heating at 70 ˚C, followed by a 10 ˚C/min ramp to 320 ˚C, and a final 2 minutes at 320 ˚C. Impact mass spectra were recorded at 70 eV, and all spectra were recorded in the mass range of 50 to 800 m/z.

- DNA extraction, amplification and sequencing

Using the DenaZist Asia fungal DNA isolation kit, total genomic DNA was extracted from fungal mycelia. To identify the selected fungus at the species level, ITS, TEF-1α, and TUB2 gene regions were amplified. All PCR reactions were performed using TopTaq PCR Master Mix kit to to ensure precise amplification in a total reaction volume of 25 µl. The PCR conditions consisted of an initial denaturation step at 94 ˚C for 5 minutes, followed by 30 cycles of 94 ˚C for 30 seconds, 58 ˚C for 20 seconds, and 72 ˚C for 30 seconds, with a final extension step of 72 ˚C for 10 minutes. The PCR products were then purified and sequenced by Marcon Co. (South Korea). A summary of all primers used in this study can be found in Table 1.

- Phylogenetic analyses

The authentic sequences from GenBank (http://www.ncbi.nlm.nih.gov) were added to the novel sequences produced in this study (Table 2), and MAFFT v. 7 (http://mafft.cbrc.jp/alignment/server/index.html) was used to align the sequences. When needed, alignment was adjusted by hand in BioEdit v. 7.0. After independently aligning each locus, Mesquite 2.75 was used to concatenate the alignments[46]. Phylogenetic analyses of single and combined alignments (ITS, TEF1-α, and TUB2), were carried out using Maximum Parsimony (MP) and Bayesian Inference (BI) algorithms. For MP analysis using PAUP v. 4.0b10 (Swofford, 2003) we followed Abdollahzadeh et al. (2013) [47,48]. MrModelTest v. 2.3 was used to identify the best nucleotide substitution models for every locus (Nylander, 2004)[49]. BI was conducted via the CIPRES Science Gateway portal (https://www.phylo.org/; Miller et al., 2012) using MrBayes v. 3.2.6 (Huelsenbeck & Ronquist 2001, Ronquist & Huelsenbeck 2003) as described by Nahvi Moghadam et al. (2022) [50–53]. FigTree v. 1.4.3 (http://tree.bio.ed.ac.uk/software/figtree) was used to show phylogenetic trees, while Adobe Illustrator CS2 v. 12.0.0 was used for editing. Taxonomic innovations have been added to MycoBank (www.MycoBank.org; Crous et al., 2004).

- Morphological characterization

Cultural characteristics were recorded on MEA, OA and PDA at room temperature (20–25 °C). Cultures were kept under mixed near-UV and cool-white fluorescent lights with a 12 -hour light-dark cycle for three to four months to promote both sexual and asexual reproductions. Microscopy and measurements based on at least 20 fungal structures were done using an Olympus BX51 microscope equipped with a Cell Sense Entry measurement module and an Olympus DP72 camera according to Nahvi Moghadam et al. (2022) [53]

## Declarations

# Funding

The University of Kurdistan, Sanandaj, Iran. The Canadian Institute for Health, Canada funded R. C. Levesque for this research.

# Author Contribution

Project management was done by B. B, R.C.L. and A. V.. Samples were prepared and gathered by S.M. Data generation and analysis were done by S.M., J.A., and S.B. Manuscript draft prepared by S.M. The work was examined and edited by all authors. The completed manuscript was read and approved by the authors.

# Acknowledgments

The authors would like to thank Dr. Jeff Gauthier for his knowledge and assistance. All processes related to plant collection for this research were carried out by Hossein Maroofi, a botanist at the Kurdistan Agricultural and Natural Resources Research and Education Center.

# Data Availability

The datasets used and/or analysed during the current study available from the corresponding author on reasonable request.• All data generated or analysed during this study are included in this published article [and its supplementary information files].

Verification and documentation of all collected plants, along with their storage under specific herbarium codes, can be accessed through this link (Herbarium Details | Kurdistan Agricultural and Natural Resources Research and Education Center (nybg.org). The herbarium code assigned to the collected *Papaver bracteatum* is 8931.

As per the regulations governing the collection of wild plants in Iran, permission was not required. However, authors comply with the IUCN Policy Statement on Research Involving Species at Risk of Extinction and the Convention on the Trade in Endangered Species of Wild Fauna and Flora. The plant collection serves as a valuable resource for botanical research, offering access to a diverse range of plant species for scientific study. Researchers can explore various fields including plant taxonomy, genetics, physiology, ecology, and other branches of botanical science, utilizing the resources provided by the collection. Additionally, regarding the results, all findings are accessible, and we are more than willing to share them upon request.

All data generated or analysed during this study are included in this published article and its supplementary information files.

# References


1. Roberts, M. F., Kutchan, T. M., Brown, R. T. & Coscia, C. J. Implication of tyramine in the biosynthesis of morphinan alkaloids in *Papaver*. *Planta* **172**, (1987).
2. Fossati, E. *et al.* Reconstitution of a 10-gene pathway for synthesis of the plant alkaloid dihydrosanguinarine in *Saccharomyces cerevisiae*. *Nat Commun* **5**, (2014).
3. Sharafı, A. *et al.* Metabolic engineering of morphinan alkaloids by over-expression of codeinone reductase in transgenic hairy roots of *Papaver bracteatum*, the Iranian poppy. *Biotechnol Lett* **35**, (2013).
4. Singh, A., Menéndez-Perdomo, I. M. & Facchini, P. J. Benzylisoquinoline alkaloid biosynthesis in opium poppy: an update. *Phytochemistry Reviews* vol. 18 Preprint at https://doi.org/10.1007/s11101-019-09644-w (2019).
5. Gurkok, T. *et al.* Functional characterization of 4'OMT and 7OMT Genes in BIA biosynthesis. *Front Plant Sci* **7**, (2016).
6. Behzadirad, M., Naghavi, M. R. & Bushehri, A. A. S. Importance of hormonal elicitors in inducing morphine biosynthesis in the cell culture of (*Papaver bracteatum* Lindl.). *Journal of Agricultural Science and Technology* **22**, (2020).
7. Allen, R. S. *et al.* RNAi-mediated replacement of morphine with the nonnarcotic alkaloid reticuline in opium poppy. *Nat Biotechnol* **22**, (2004).
8. Labanca, F., Ovesnà, J. & Milella, L. Papaver somniferum L. taxonomy, uses and new insight in poppy alkaloid pathways. *Phytochemistry Reviews* **17**, (2018).
9. Shaghaghi, A., Alirezalu, A., Nazarianpour, E., Sonboli, A. & Nejad-Ebrahimi, S. Opioid alkaloids profiling and antioxidant capacity of *Papaver* species from Iran. *Ind Crops Prod* **142**, (2019).
10. Mozaffarian, V. *A Dictionary of Iranian Plant Names*. *Farhang Moaser. Tehran* (1996).
11. Carroll, G. Fungal endophytes in stems and leaves: from latent pathogen to mutualistic symbiont. *Ecology* **69**, (1988).
12. Redman, R. S., Sheehan, K. B., Stout, R. G., Rodriguez, R. J. & Henson, J. M. Thermotolerance generated by plant/fungal symbiosis. *Science* vol. 298 Preprint at https://doi.org/10.1126/science.1072191 (2002).
13. Miller, J. D., Mackenzie, S., Foto, M., Adams, G. W. & Findlay, J. A. Needles of white spruce inoculated with rugulosin-producing endophytes contain rugulosin reducing spruce budworm growth rate. *Mycol Res* **106**, (2002).

14. Porras-Alfaro, A. *et al.* Novel root fungal consortium associated with a dominant desert grass. *Appl Environ Microbiol* **74**, (2008).
15. Schmidt, R. *et al.* Effects of bacterial inoculants on the indigenous microbiome and secondary metabolites of chamomile plants. *Front Microbiol* **5**, (2014).
16. Stierle, A., Strobel, G. & Stierle, D. Taxol and taxane production by *Taxomyces andreanae*, an endophytic fungus of Pacific yew. *Science (1979)* **260**, (1993).
17. Kusari, S., Hertweck, C. & Spiteller, M. Chemical ecology of endophytic fungi: Origins of secondary metabolites. *Chemistry and Biology* vol. 19 Preprint at https://doi.org/10.1016/j.chembiol.2012.06.004 (2012).
18. Puri, S. G., Verma, V., Amna, T., Qazi, G. N. & Spiteller, M. An endophytic fungus from *Nothapodytes foetida* that produces camptothecin. *J Nat Prod* **68**, (2005).
19. Cui, Y. *et al.* Ginkgolide B produced endophytic fungus (*Fusarium oxysporum*) isolated from Ginkgo biloba. *Fitoterapia* **83**, (2012).
20. Patil, R. H., Patil, M. P. & Maheshwari, V. L. Bioactive Secondary Metabolites From Endophytic Fungi: A Review of Biotechnological Production and Their Potential Applications. in *Studies in Natural Products Chemistry* vol. 49 (2016).
21. Owen, N. L. & Hundley, N. Endophytes--the chemical synthesizers inside plants. *Science progress* vol. 87 Preprint at https://doi.org/10.3184/003685004783238553 (2004).
22. Dubey, A., Malla, M. A., Kumar, A., Dayanandan, S. & Khan, M. L. Plants endophytes: unveiling hidden agenda for bioprospecting toward sustainable agriculture. *Critical Reviews in Biotechnology* vol. 40 Preprint at https://doi.org/10.1080/07388551.2020.1808584 (2020).
23. Tiwari, P. & Bae, H. Horizontal gene transfer and endophytes: An implication for the acquisition of novel traits. *Plants* vol. 9 Preprint at https://doi.org/10.3390/plants9030305 (2020).
24. Tan, R. X. & Zou, W. X. Endophytes: A rich source of functional metabolites. *Natural Product Reports* vol. 18 Preprint at https://doi.org/10.1039/b100918o (2001).
25. Tazik, Z. *et al.* LC-MS based identification of stylosin and tschimgine from fungal endophytes associated with *Ferula ovina*. *Iran J Basic Med Sci* **23**, (2020).
26. Von Arx, J. A. Ostiolate and nonostiolate pyrenomycetes. *Proceedings of the Koninklijke Nederlandse Akademie van Wetenschappen - Series C* **76**, (1973).
27. Malloch, D. & Hubart, J. M. An undescribed species of *Microascus* from the Cave of Ramioul. *Canadian Journal of Botany* **65**, (1987).
28. Abbott, S. P., Lumley, T. C. & Sigler, L. Use of holomorph characters to delimit *Microascus nidicola* and *M. soppii* sp. nov., with notes on the genus *Pithoascus*. *Mycologia* **94**, (2002).
29. Guarro Josep, Gené Josepa, Stchigel M Alberto & Figueras M José. Atlas of soil *ascomycetes*. *No Title* (2012).
30. Sandoval-Denis, M. *et al.* Redefining Microascus, Scopulariopsis and allied genera. *Persoonia: Molecular Phylogeny and Evolution of Fungi* **36**, (2016).
31. Jagielski, T. *et al.* Molecular taxonomy of *scopulariopsis*-like fungi with description of new clinical and environmental species. *Fungal Biol* **120**, (2016).
32. Tazik, Z., Rahnama, K., Iranshahi, M., White, J. F. & Soltanloo, H. A new species of *Pithoascus* and first report of this genus as endophyte associated with *Ferula ovina*. *Mycoscience* **61**, (2020).
33. El-Desoky, N. I., Hashem, N. M., Gonzalez-Bulnes, A., Elkomy, A. G. & Abo-Elezz, Z. R. Effects of a nanoencapsulated moringa leaf ethanolic extract on the physiology, metabolism and reproductive performance of rabbit does during summer. *Antioxidants* **10**, (2021).
34. Hrideek, T. K., Ginu, J., Raghu, A. V. & Jijeesh, C. M. Phytochemical profiling of bark and leaf volatile oil of two wild cinnamomum species from evergreen forests of Western Ghats. *Plant Arch* **16**, (2016).

35. Kuiate, J. R., Bessière, J. M., Zollo, P. H. A. & Kuate, S. P. Chemical composition and antidermatophytic properties of volatile fractions of hexanic extract from leaves of *Cupressus lusitanica Mill.* from Cameroon. *J Ethnopharmacol* **103**, (2006).
36. Forouzesh, A., Zand, E., Soufizadeh, S. & Samadi Foroushani, S. Classification of herbicides according to chemical family for weed resistance management strategies-an update. *Weed Res* **55**, (2015).
37. Muthukumaran, P., Kumaravel, S. & Nimia, N. Phytochemical, GC-MS and FT-IR Analysis of *Papaver somniferum* L. *Journal of Pharmaceutical and Biological Sciences* **7**, (2019).
38. Ancheeva, E., Daletos, G. & Proksch, P. Bioactive Secondary Metabolites from Endophytic Fungi. *Curr Med Chem* **27**, (2019).
39. Quesada-Moraga, E., Landa, B. B., Muñoz-Ledesma, J., Jiménez-Diáz, R. M. & Santiago-Álvarez, C. Endophytic colonisation of opium poppy, *Papaver somniferum*, by an entomopathogenic *Beauveria bassiana* strain. *Mycopathologia* **161**, (2006).
40. Ray, T. *et al.* Molecular insights into enhanced resistance of Papaver somniferum against downy mildew by application of endophyte bacteria Microbacterium sp. SMR1. *Physiol Plant* **173**, (2021).
41. Rehman, H. ur. Biological screening of endophytic fungi extracted from different parts of medicinal plants. *Pure and Applied Biology* **9**, (2020).
42. Cauchi, M. *et al.* Comparison of GC-MS, HPLC-MS and SIFT-MS in conjunction with multivariate classification for the diagnosis of Crohn's disease in urine. *Analytical Methods* **7**, (2015).
43. Wang, Y. *et al.* Metabolomic analysis with GC-MS to reveal potential metabolites and biological pathways involved in Pb &cd stress response of radish roots. *Sci Rep* **5**, (2015).
44. Pyne, M. E., Narcross, L. & Martin, V. J. J. Engineering plant secondary metabolism in microbial systems. *Plant Physiol* **179**, (2019).
45. de Falco, B., Fiore, A., Rossi, R., Amato, M. & Lanzotti, V. Metabolomics driven analysis by UAEGC-MS and antioxidant activity of chia (*Salvia hispanica L.*) commercial and mutant seeds. *Food Chem* **254**, (2018).
46. Maddison WP & Maddison DR. a modular system for evolutionary analysis version 3.51 [Internet]. http://mesquiteproject.org. (2018).
47. Swofford DL. PAUP^* Phylogenetic Analysis Using Parsimony (^* and Other Methods). Version 4. *http://paup. csit. fsu. edu/* (2003).
48. Abdollahzadeh, J., Zare, R. & Phillips, A. J. L. Phylogeny and taxonomy of Botryosphaeria and Neofusicoccum species in Iran, with description of Botryosphaeria scharifii sp. Nov. *Mycologia* **105**, (2013).
49. Nylander, J. A. MrModeltest 2. Program distributed by the author. Evolutionary Biology Centre, Uppsala University. *Evolutionary Biology Centre Uppsala University* (2004).
50. Miller, M. A., Pfeiffer, W. & Schwartz, T. The CIPRES science gateway: Enabling high-impact science for phylogenetics researchers with limited resources. in *ACM International Conference Proceeding Series* (2012). doi:10.1145/2335755.2335836.
51. Huelsenbeck, J. P. & Ronquist, F. MRBAYES: Bayesian inference of phylogenetic trees. *Bioinformatics* **17**, (2001).
52. Ronquist, F. & Huelsenbeck, J. P. MrBayes 3: Bayesian phylogenetic inference under mixed models. *Bioinformatics* **19**, (2003).
53. Moghadam, J. N., Khaledi, E., Abdollahzadeh, J. & Amini, J. Seimatosporium marivanicum, Sporocadus kurdistanicus, and Xenoseimatosporium kurdistanicum: three new pestalotioid species associated with grapevine trunk diseases from the Kurdistan Province, Iran. *Mycol Prog* **21**, (2022).

# Tables

**Table 1**. Primers are used for PCR amplification and sequencing.

| Gene | Primer | | Product size [bp] | Ta°C |
|---|---|---|---|---|
| | Designation | Nucleotide sequence | | |
| ITS | ITS1 | 5'-CTTGGTCATTTAGAGGAAGTAA-3' | 1500 | 53 |
| | ITS4 | 5'-TCCTCCGCTTATTGATATGC-3' | | |
| TUB | BT2a | 5'-GGTAACCAAATCGGTGCTGCTTTC-3' | 550 | 55 |
| | BT2b | 5'-ACCCTCAGTGTAGTGACCCTTGGC-3' | | |
| EF | 983F | 5'-GCy[1]CCy[1]GGhCAy[1]CGTGAy[1]TTy[1]AT-3' | 1000 | 65 |
| | 2218R | 5'-ATGACACCr[1]ACr[1]GCr[1]ACr[1]GTy[1]TG-3' | | |

[1]Degenerate nucleotides: y, C or T; h, A, C, or T; r, A or G.

**Table 2.** Strains used in phylogenetic analyses.

| Species | Isolate No.1 | Host | Location | GenBank accession number2 | | |
|---|---|---|---|---|---|---|
| | | | | ITS | TUB2 | EF1-α |
| *Pithoascus kurdistanensis* | IRAN 4653C T | *Papaver bracteatum* | Iran | OR224479 | OR215044 | OR221070 |
| *Pithoascus intermedius* | CBS 217.32T | Root of *Fragaria vesca* | USA | LM652450 | LM652662 | LM652579 |
| *Pithoascus nidicola* | CBS 197.61T | *Dipodomys merriami* | USA | LM652451 | LM652663 | LM652580 |
| *Pithoascus exsertus* | CBS 819.70T | *Megachile willoughbiella* | Denmark | LM652449 | LM652578 | LM652661 |
| *Pithoascus ater* | CBS 400.34T | Unknown | Unknown | LM652447 | LM652659 | LM652576 |
| *Pithoascus lunatus* | CBS 103.85T | Skin (*Tinea plantaris*) | Germany | LN850784 | LN850881 | LN850929 |
| *Pithoascus stoveri* | CBS 176.71T | Root of *Beta vulgaris* | USA | LM652453 | LM652664 | LM652581 |
| *Pithoascus persica* | IRAN 3309C | Root of *Ferula ovina* | Iran | MF186873 | - | MK430530 |
| *Wardomycopsis inopinata* | FMR 10305 | Soil | Myanmar | LM652498 | LN851160 | LN851106 |
| *Pseudoscopulariopsis schumacheri* | CBS 435.86T | soil | Spain | LM652455 | LM652666 | LM652583 |
| *Microascus longirostris* | CBS 196.61NT | Wasp's nest | USA | LM652421 | LM652634 | LM652566 |
| *Microascus croci* | CBS 296.61T | Air | Brazil | LM652408 | LM652622 | LM652561 |
| *Microascus gracilis* | CBS 369.70T | Food | Japan | LM652412 | LM652625 | HG380390 |
| *Scopulariopsis cordiae* | CBS 138129T | Human finger | USA | LM652491 | LM652673 | HG380422 |
| *Wardomycopsis humicola* | CBS 487.66T | Soil | Canada | LM652497 | LN851157 | LN851103 |
| *Scopulariopsis brevicaulis* | UTHSC 07-1812 | Human toenail | USA | LM652470 | LM652677 | HG380366 |
| *Gamsia aggregata* | CBS 251.69T | Dung of carnivore | USA | LM652378 | LN851144 | LN851090 |
| *Lophotrichus macrosporus* | NBRC 32894* | Sheep dung | Iraq | 3289401* | - | - |
| *Lophotrichus plumbescens* | NBRC 30864T* | Soil | Thailand | 03086401* | - | - |
| *Kernia nitida* | CBS 282.52 | *Chrysolina sanguinolenta* | France | MH857035 | MN982415 | MN982407 |
| *Kernia pachypleura* | CBS | Soil of paddy | Japan | MH859937 | MN982417 | MN982410 |

| | | | | | | |
|---|---|---|---|---|---|---|
| | 776.70 | field | | | | |
| *Scedosporium aurantiacum* | CBS 116910 | Ulcer of ankle | Spain | HQ231818 | - | - |
| *Scedosporium boydii* | CBS 330.93 | Bronchial secretion | Netherlands | AY863196 | - | - |
| *Petriella sordida* | CBS 124169 | Corner of a bathroom | Netherlands | GQ426957 | - | - |
| *Petriellopsis africana* | CBS 311.72T | Brown sandy soil | Namibia | AJ888425 | - | - |
| *Trichoderma asperellum* | NBRC 101777T* | sclerotia of *Sclerotinia minor* | USA | 11776302* | - | - |
| *Petriella setifera* | CBS. 391.75 | infection of dolphin | Netherlands | AY882344 | | - |
| *Microascus murinus* | CBS 830.70T | Composed municipal waste | Germany | LM652424 | LM652637 | HG380404 |
| *Yunnania carbonaria* | CBS 205.61T | Soil | Panama | LM652489 | LM652695 | HG380385 |
| *Fairmania singularis* | CBS 414.64 | Laboratory contaminant | Japan | LM652442 | LN851088 | LN851142 |
| *Cephalotrichum asperulum* | CBS 127.22 | Seed | Netherlands | LN850959 | LN851113 | LN851060 |
| *Gamsia columbina* | CBS 546.69T | Milled *Oryza sativa* | Japan | LM652379 | LN851148 | LN851094 |
| *Acaulium acremonium* | MUCL 8274 | Wheat field soil | Germany | LM652457 | LN851109 | LN851056 |
| *Acaulium acremonium* | MUCL 8409 | Soil | Germany | LM652458 | LN851110 | LN851057 |
| *Acaulium acremonium* | CBS 290.38T | Skin of a horse | Denmark | LM652456 | LN851108 | HG380362 |
| *Cephalotrichum cylindricum* | CBS 448.51 | Timber | South Africa | LN850964 | LN851118 | LN851065 |
| *Wardomyces inflatus* | CBS 216.61T | Wood, *Acer* sp. | Canada | LM652496 | LN851152 | LN851098 |
| *Parascedosporium tectonae* | CBS 127.84T | Seed | Jamaica | AY228113 | - | EF151409 |
| *Wardomyces giganteus* | CBS 746.69T | Insect frass in dead log | Canada | LM652411 | LN851150 | LN851096 |

1CBS Culture collection of the Westerdijk Fungal Biodiversity Institute, Utrecht, The Netherlands; FMR: Facultat de Medicina i Ciències de la Salut, Reus, Spain; FMR: Facultat de Medicina i Ciències de la Salut, Reus, Spain; NBRC: National

Biological Resource Centre, Japan; UAMH: University of Alberta Microfungus Collection and Herbarium, Canada; UTHSC: Fungus Testing Laboratory, Department of Pathology, University of Texas Health Science Center, San Antonio, USA

2ITS: Internal transcribed spacer of the rDNA and 5.8S regions; EF-1α: partial translation elongation factor gene; TUB2: partial beta-tubulin gene. * Sequences obtained from the NBRC database.

**Table 3**. HPLC analysis for the presence of the morphinan alkaloids in fungi isolates (Mg/g).

| Fungi isolates | Morphine | Codeine | Papaverine | Thebaine |
|---|---|---|---|---|
| BR4 | 2.76 | 0.16 | -- | -- |
| BR6 | 23.06 | 2.03 | -- | -- |
| GR1 | 9.12 | -- | -- | -- |
| GR4 | 13.81 | 0.38 | -- | -- |
| PR1 | 4.26 | 0.18 | -- | -- |
| PS1 | 5.73 | 0.49 | -- | -- |

**Tables 4**. GC-MS analysis revealed the presence of bioactive compounds in the BR6.

| S. No | Name of the compound | Ret time | Identified Compound Details | Molecular Formula |
|---|---|---|---|---|
| 1 | Dibutyl phthalate | 24.508 | Organic compound, ester compound, plasticizer | C16H22O4 |
| 2 | Bis(2-ethylhexyl) phthalate | 24.508 | Organic compound, phthalates, plasticizer in medical devices | C24H38O4 |
| 3 | 3-OXO-18-NOR-ENT-ROS-4-ENE-15. beta.,16 Acetonide | 24.508 | Organic compound, Antifeedent, antiviral | C22H34O3 |
| 4 | 1,2-Benzenedicarboxylic acid, 3-phenoxy | 24.508 | Organic compound, ester compound, plasticizer | C14H10O5 |
| 5 | Ethofumesate | 24.110 | Organic compound, ester, and a member of 1-benzofurans. ester and a member of 1-benzofurans. herbicide. | C13H18O5S |
| 6 | Benzylideneacetone | 24.508 | Organic compound, ketone, flavoring ingredient in food and perfumes, | C10H10O |
| 7 | 2-Ethylacridine | 24.110 | Organic compound, Antimicrobial and antitumor, antioxidant activity | C15H13N |
| 8 | 4H-Pyrane-3-carboxamide | 24.110 | Organic compound, heterocyclic compounds, pharmacological activities, such as spasmolytic, diuretic, anticoagulant, anticancer, and anti anaphylactic activity | C6H6O3 |
| 9 | 1,3-dimethyl-4-azaphenanthrene | 24.110 | Organic compound, Polycyclic aromatic hydrocarbons, potent toxic environmental pollutants with carcinogenic properties | C15H13N |
| 10 | Codeine | 23.565 | Organic compound, plant alkaloids, opiate and prodrug of morphine used to treat pain, coughing, and diarrhea | C18H21NO3 |
| 11 | Morphinan-6-ol, 7,8-didehydro-4,5-epoxy-17-methyl-3-(phenylmethoxy)-, (5alpha,6alpha)- | 23.565 | Organic compound, plant alkaloids, opiate analgesic psychoactive drug | C24H25NO3 |
| 12 | Papaverine | 22.09 | Organic compound, opium alkaloid, an antispasmodic drug | C20H21NO4 |
| 13 | Ethidimuron | 22.222 | Organic Chemicals, Methylurea Compounds, herbicide, and pesticide | C7H12N4O3S2 |
| 14 | Hexadecanoic acid | 18.796 | Organic compound, fatty acid found in animals, plants, and microorganisms, food additive, and emollient or surfactant in cosmetics. | C16H32O2 |
| 15 | Pentadecanoic acid | 18.796 | Organic compound, a saturated fatty acid, has a role as a plant metabolite, a food component, a Daphnia Magna metabolite, a human blood serum metabolite, and an algal metabolite | C15H30O2 |
| 16 | Vamidothion | 18.796 | Organic compound, organic thiophosphate, insecticide and acaricide | C8H18NO4PS2 |

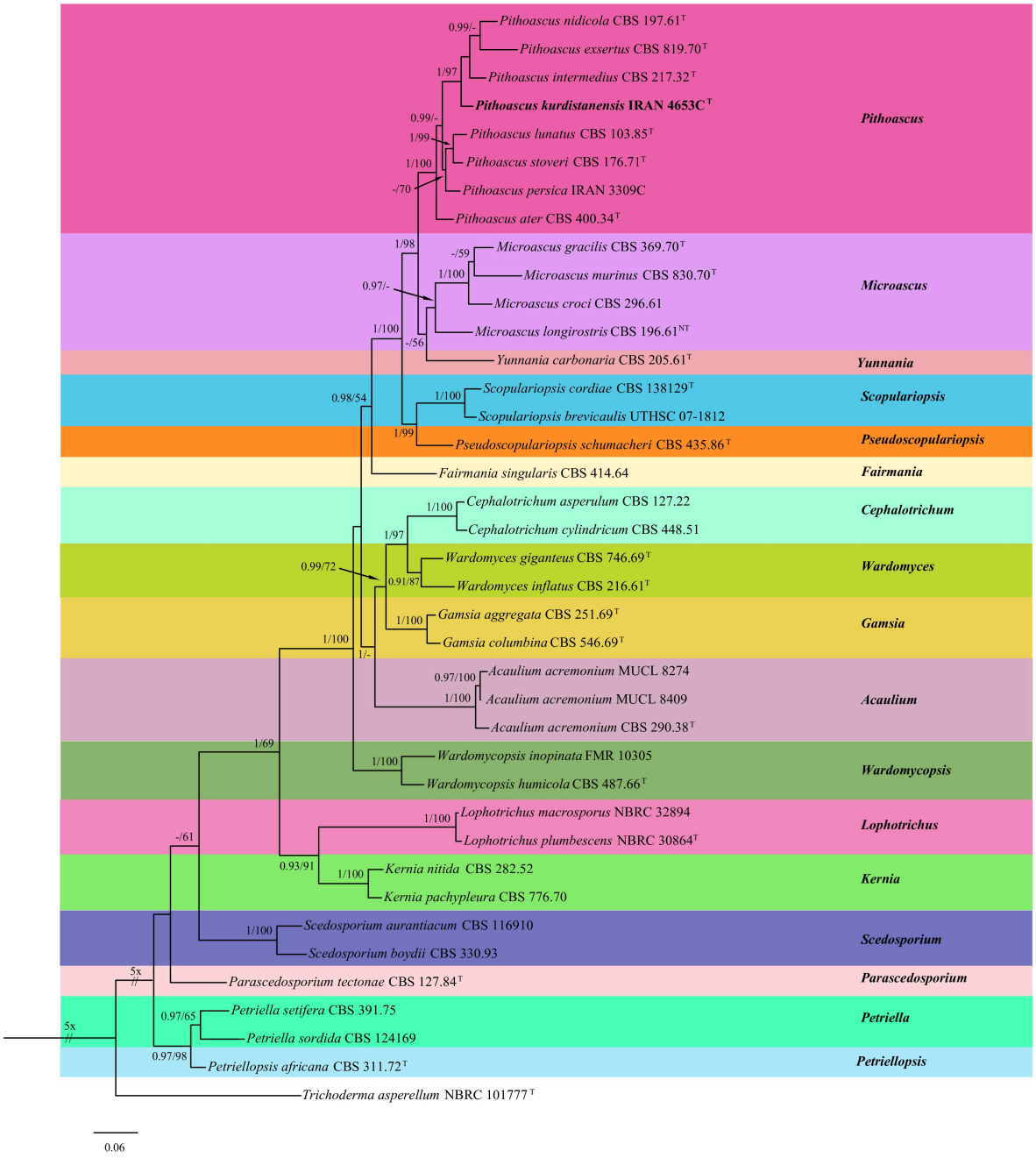
| | | | | |
|---|---|---|---|---|
| 17 | Dimethoate | 18.796 | Organic compound. monocarboxylic acid amide, insecticide, and on several field-grown agricultural crops | C5H12NO3PS2 |
| 18 | Demephion | 18.796 | Organic compound, organothiophosphate, insecticide | C10H26O6P2S4 |
| 19 | Octadecane | 17.478 | organic compound, alkane hydrocarbon, used as a solvent, lubricant, transformer oil, and anti-corrosion agents | C18H38 |
| 20 | Eicosane | 16.391 | Organic compound, alkane, use in the petrochemical industry | C20H42 |
| 21 | Trimethylsilyl [2-(4-chlorophenyl)-4-phenyl-1,3-thiazol-5-yl]acetate | 16.727 | Unknown | |
| 22 | Trimethylsilyl 3-methoxy-2-(2-oxo-2-((trimethylsilyl)oxy)ethoxy)benzoate | 16.727 | Organic compound, No activity reported | C16H26O6Si2 |
| 23 | Hexasiloxane, tetradecamethyl | 16.727 | Organic compound, No activity reported | C14H42O5Si6 |
| 24 | Heptadecane | 16.391 | Organic compound, an alkane hydrocarbon, role as a plant metabolite and a volatile oil component | CH□(CH□)□□CH□ |
| 25 | Eicosane | 16.391 | Organic compound, an alkane, used in cosmetics, lubricants, plasticizers, and in the petrochemical industry. | C20H42 |
| 26 | Bicyclo[4.4.0]dec-1-ene, 2-isopropyl-5-methyl-9-methylene- | 15.263 | Organic compound, No activity reported | C15H24 |
| 27 | isoledene | 15.263 | Organic compound, No activity reported | C15H24 |
| 28 | delta.-Cadinene Naphthalene | 15.923 | Organic compound, essential oils, antibacterial | C15H24 |
| 28 | Epi-bicyclosesquiphellandrene | 15.765 | Organic compound, sesquiterpenoids, antimicrobial | C15H24 |
| 30 | Gamma-Cadinene | 15.849 | Organic compound, essential oils, sesquiterpenoids, antibacterial | C15H24 |

**Table 5**. Main morphological features for discriminating *Pithoascus* species.

| Species | Conidia | | Ascospores size | Asci | | Ascocarps | | Reference |
|---|---|---|---|---|---|---|---|---|
| | size (µm) | arrangement | (µm) | size (µm) | shape | size (µm) | ostiole | |
| P. ater | 4–9 × 4.5–8.5 | Solitary | Nr* | Nr* | Nr* | Nr* | Nr* | Sandoval-Denis et al., 2016 |
| P. exsertus | Nr* | Nr* | 6.7–12 × 1.3–2.5 | 10–18.5 × 4–7.5 | cylindrical to barrel | 213–438 | + | Skou 1973 |
| P. intermedius | 4–8 × 4.5–7.5 | Solitary | 5–6 × 2–2.5 | 11–15 × 7–9 | ellipsoid/clavate | 120–200 | + | Doveri 2011 |
| P. kurdistanensis | 3.3–5.7 × 2.8–4.5 | Chain | 4.8–6.1 × 1.6–2.5 | 5–10 | globose | 67–243 | - | This study |
| P. lunatus | Nr* | Nr* | 5–5.5 × 2.5 | 9.5–12.5 × 5–9 | subglobose to ellipsoid | 111–143 | + | Jagielski et al., 2016 |
| P. nidicola | 4–5 × 2.5–3.5 | Solitary | 6–8 × 2–2.5 | 10–15 × 7–12 | ellipsoid to barrel | 90–160 | + | von Arx 1973; Sandoval-Denis et al., 2016 |
| P. persica | 4–5 | Chain | 6.5–8 × 3.5–3.8 | Nr* | Nr* | 200–260 | - | Tazik et al. 2020 |
| P. stoveri | 5–8 × 3–4 | Solitary | 6–7.5 × 2–3 | 11–15 × 7–10 | ellipsoid to barrel | 50–110 | - | von Arx 1973; Sandoval-Denis et al., 2016 |

*: Not reported

## Figures




## Figure 1

Bayesian analysis of a concatenated alignment of ITS, TEF-1α, and TUB2 yielded the phylogenetic tree. At each node, the maximum parsimony bootstrap support values (MP) and Bayesian posterior probabilities (PP) are displayed (PP/MP). Ex-type strains are indicated with T. The scale bar represents the expected number of changes per site. The tree was rooted to *Trichoderma asperellum* (NBRC 101777).

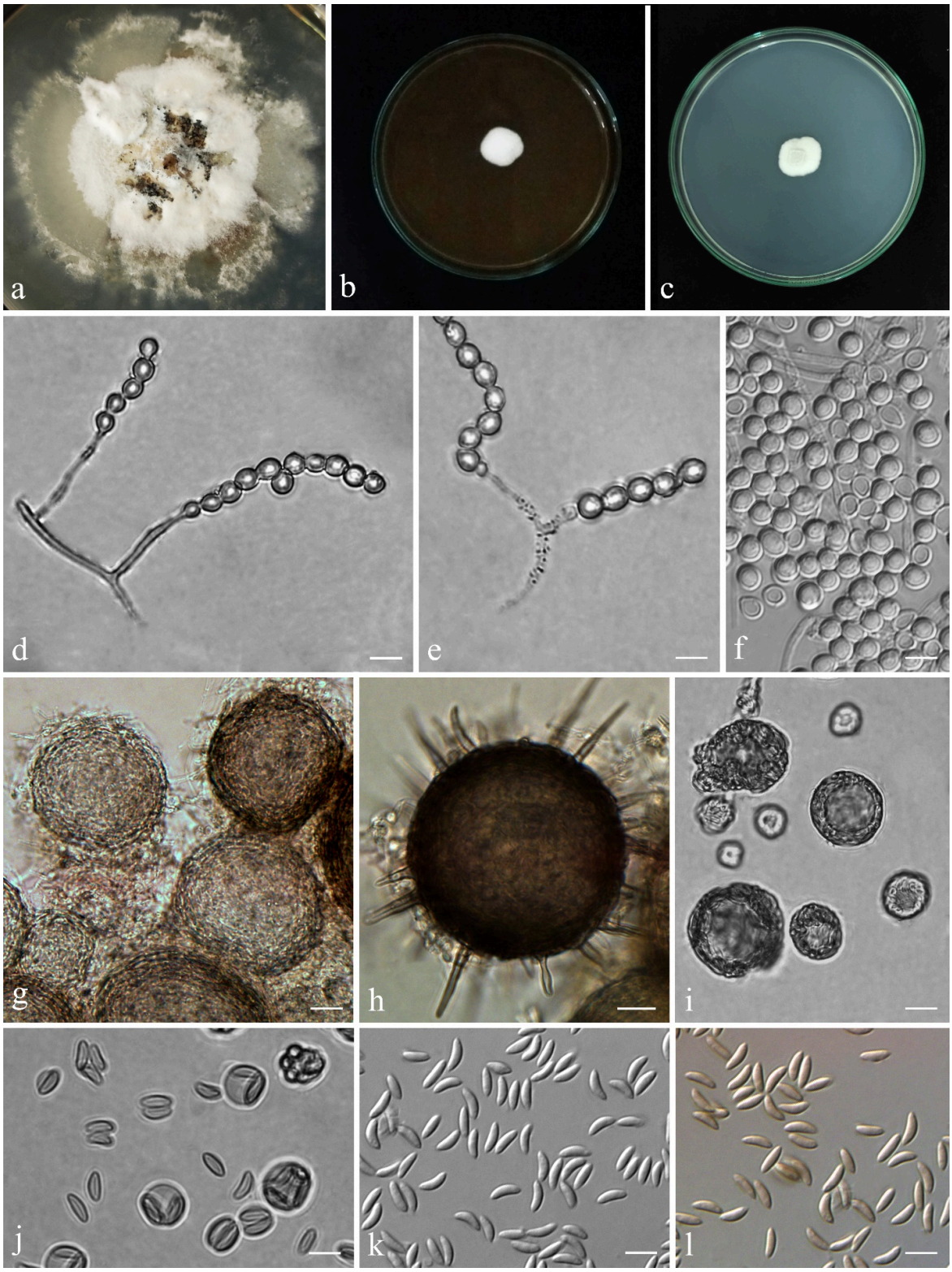



**Figure 2**

*Pithoascus kurdistanensis*: (a–c) colonies on PDA (4-wk-old), MEA (2-wk-old) and OA (2-wk-old); (d, e) conidial long basipetal chain on conidiogenous cells; (f) hyaline, aseptate conidia; (g) immature ascomata; (h) mature ascomata with setae; (i) round compact masses of ascospores outside asci; (j) globose 8-spored asci; (k, l) mature ascospores. Scale bars: d–f, j–l = 5 µm; g–i = 10 µm.

## Supplementary Files

This is a list of supplementary files associated with this preprint. Click to download.

- FigS1ITS.pdf
- FigS2TEF.pdf
- FigS3TUB.pdf